Plasmas in Astrophysics, Space and the Laboratory:

a context for the Triniti Collaboration

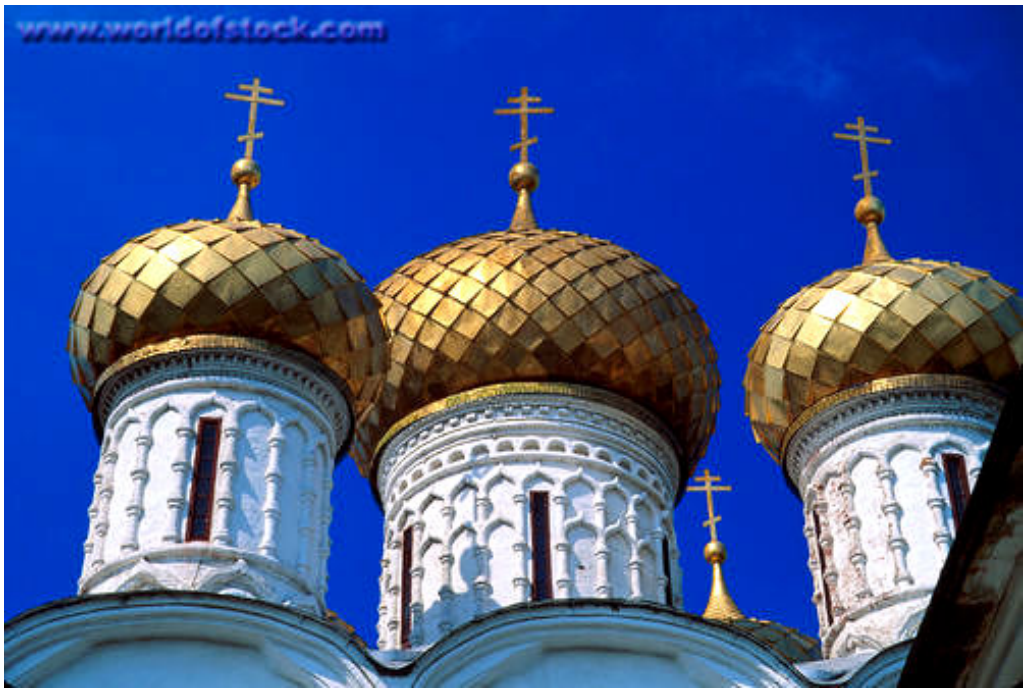

Moscow, June 2011

Why pursue research on nuclear fusion

- scientific curiosity: to see how a “lit” fusion reactor would look like and behave
- discovering basic physical processes of high energy plasmas
- generating an important connection among laboratory tested physics, observations in high energy astrophysics and space physics experiments
- developing attractive neutron sources for a variety of applications
- pioneering new advanced technologies such as very high field magnets, novel high temperature superconductors, innovative laser applications, structural materials etc.
- accessing a new source of useful energy (a DT reactor has to be close to ignition conditions in order to be capable of producing net energy)

Examples of Discoveries by Nuclear Fusion Research Relevant to Astrophysics and Space Physics

- Particle and Angular Momentum Transport due to Collective Modes (not represented by diffusion equations but by composite equations involving for instance a diffusion and an opposite “inflow” process)
- Global Self-Organization Processes determining for instance temperature and velocity profiles (e.g. considering only local effects of collective modes is not sufficient to interpret the experiments). In fact, the “Principle of Profile Consistency” (title of the original paper) should be applied to accretion structures around compact objects
- The Spontaneous Rotation Phenomenon (axisymmetric plasmas are observed to rotate spontaneously without an active injection of angular momentum)
- In depth (although not complete yet) understanding of Magnetic Reconnection processes in plasmas with non-vanishing magnetic fields and various degrees of collisionalities
- Two and Tri-dimensional Plasma and Field Configurations under nearly stationary conditions (e.g. applicable to shining black holes)

Shining Black Holes: Associated Plasma and Field Configurations

B. Coppi

M.I.T.

Moscow, June 2011

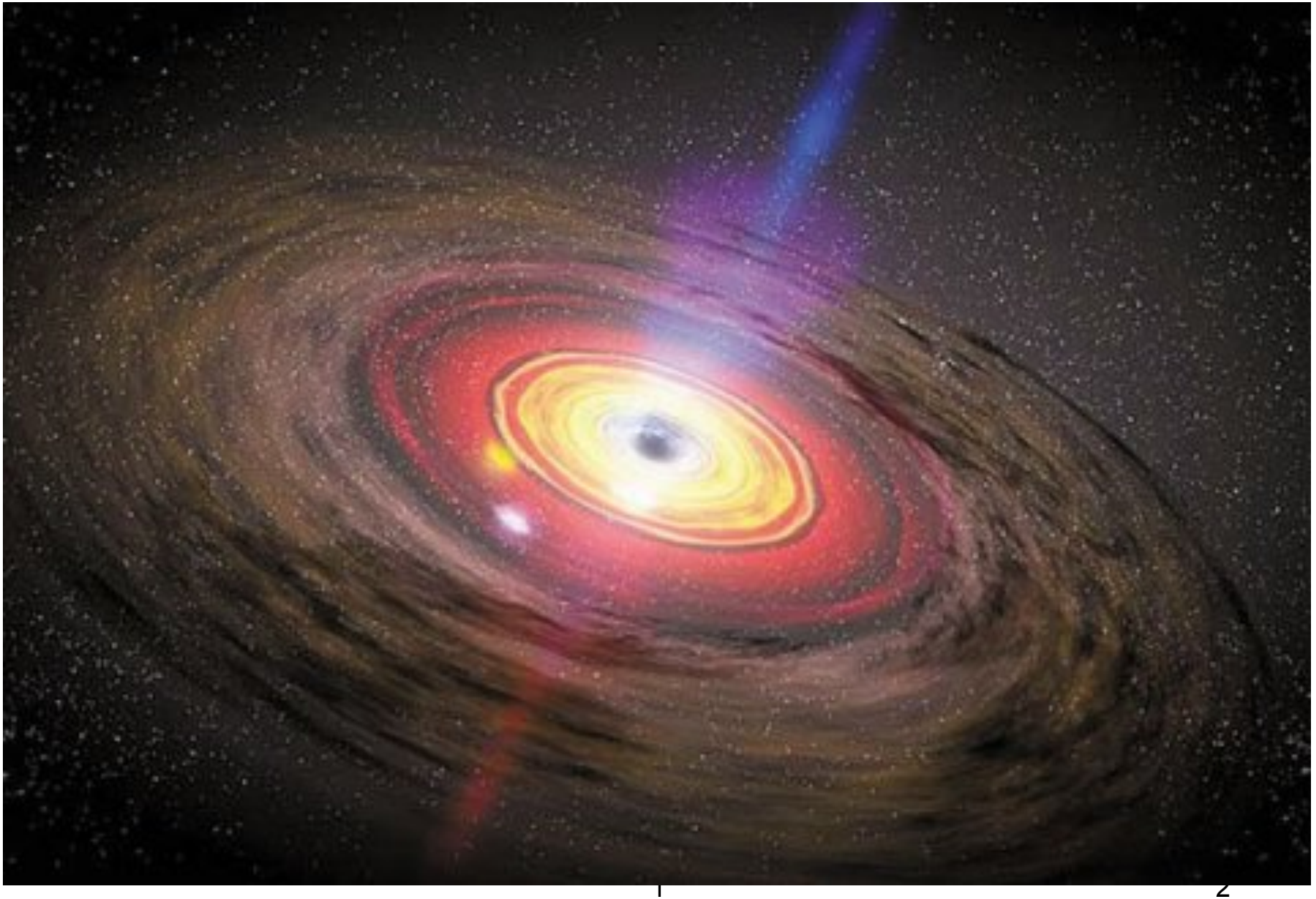

Plasma and Field Configurations

Conventional currentless disks can evolve into current carrying structures that can be axisymmetric or tridimensional

• Non-linear **Axisymmetric** (stationary) **Structures** found theoretically consist of
- Periodic Sequences of (plasma) Rings
- Solitary Ring Pairs

• **Tridimensional Structures** found in the linearized approximation consist of
- Localized Trailing Spirals

Note

• Two of the observed plasma "states" around black holes ("Thermal" and "Jet" state) can be associated with axisymmetric configurations

• One ("Extreme" state, exhibiting High-Frequency-Quasi-Periodic-Oscillations") has to be associated with non-axisymmetric configurations

Brief Comment on Pulsar Models

In dealing with axisymmetric pulsar magnetospheres we have to take

$$\mathbf{B} \simeq \frac{1}{R}\left[\nabla\psi \times \mathbf{e}_\phi + I(\psi, z)\mathbf{e}_\phi\right]$$

as poloidal currents producing slowing down $\left[\omega_0 = \omega_0(t)\right]$ have to be present. That is, I is not a function of ψ only and is an odd function of z. The relevant magnetic configuration equation was derived originally in 1971 (published in Ap. J., 1973).

In this case the magnetic force $\mathbf{F}_M$ is given by

$$\mathbf{F}_M = \frac{1}{c}\mathbf{J}\times\mathbf{B} = -\frac{1}{4\pi R^2}\left\{(\Delta_*\psi)\nabla\psi + I\nabla I - (\nabla I \times \nabla\psi)\right\}$$

and has a **toroidal** component. Here $\Delta_*\psi \equiv R\dfrac{\partial}{\partial R}\left(\dfrac{1}{R}\dfrac{\partial\psi}{\partial R}\right) + \dfrac{\partial^2}{\partial z^2}\psi$.

Two-dimensional Plasma and Field Configurations Around Black Holes

General Relativity corrections are neglected at first. The plasma is rotating around a central object with a velocity

$$V_\phi = R\Omega(R, z)$$

where

$$\Omega(R, z) \simeq \Omega_k(R) + \delta\Omega(R, z) \ ,$$

$\Omega_k \equiv \left(GM_*/R^3\right)^{1/2}$ is the Keplerian frequency for the central object of mass M_* and whose gravity is prevalent (that is, the plasma self gravity can be neglected) and $|\delta\Omega|/\Omega_k < 1$. We assume, for simplicity that $I = I(\psi)$. Then

$$\mathbf{F}_{Mp} == -\frac{1}{4\pi R^2}\left\{(\Delta_*\psi) + I\frac{dI}{d\psi}\right\}\nabla\psi,$$

as in cases considered earlier of magnetically confined plasmas.

$$\psi \simeq \psi_0(R) + \psi_1(R, z)$$

$$\Omega = \Omega(\psi)$$

Ring Sequence Solution (Periodic)

$$\psi_1 \propto N(R_*)\exp\left(-\frac{z^2}{2\Delta_z^2}\right)$$

$$\rho \propto D_*(R_*)\exp\left(-\frac{z^2}{2\Delta_z^2}\right)$$

$$C_0 \equiv \frac{\Delta_R^2}{\Delta_z^2} \ll 1\,, \qquad R_* \equiv \frac{R - R_0}{\Delta_R}$$

$$N(R_*) = \sin R_* + \frac{\varepsilon_*}{2}\sin 2R_*\,, \quad \varepsilon_* \lesssim \frac{1}{4}$$

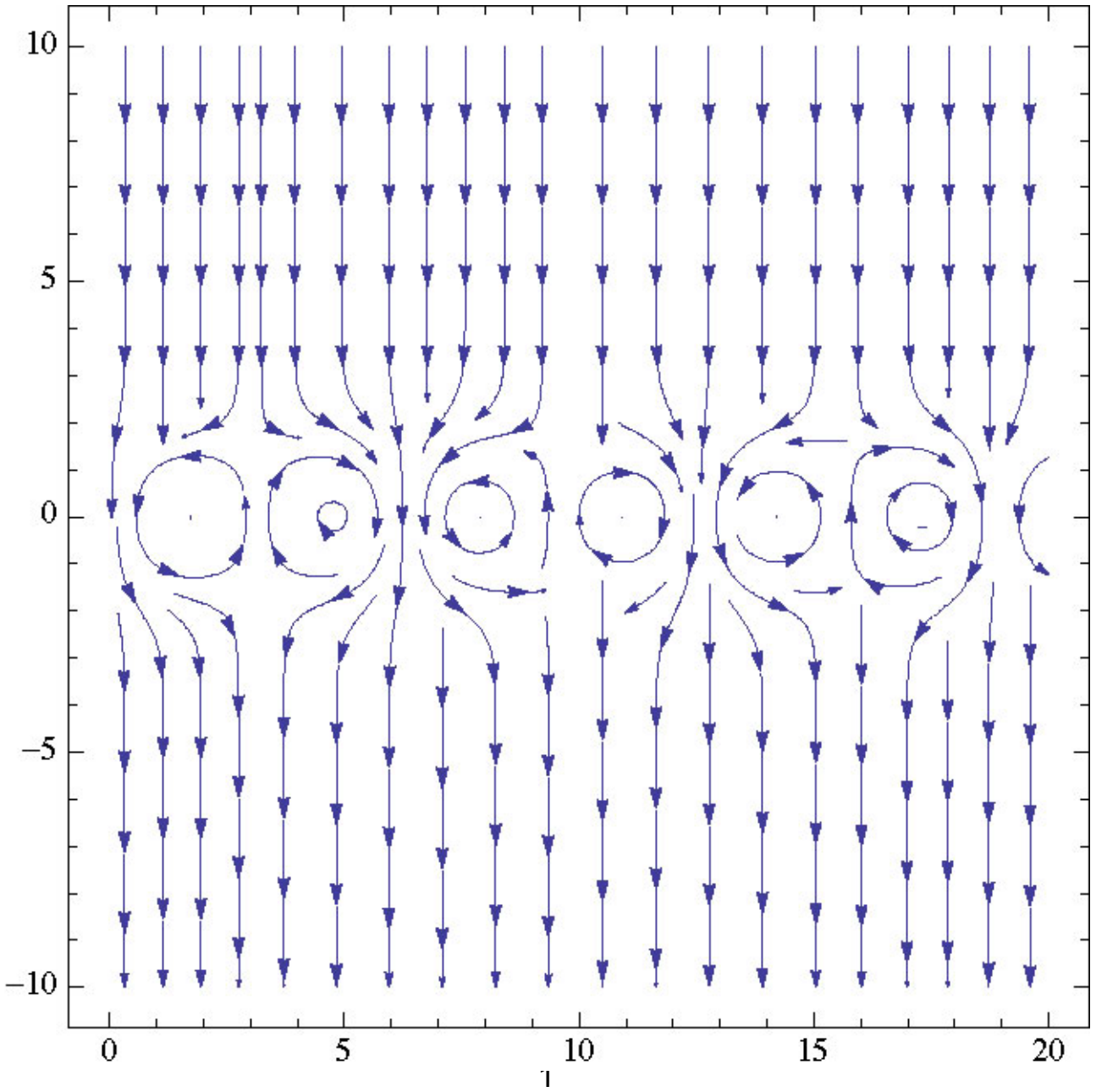
10
5
0
−5
−10
0
5
10
15
20

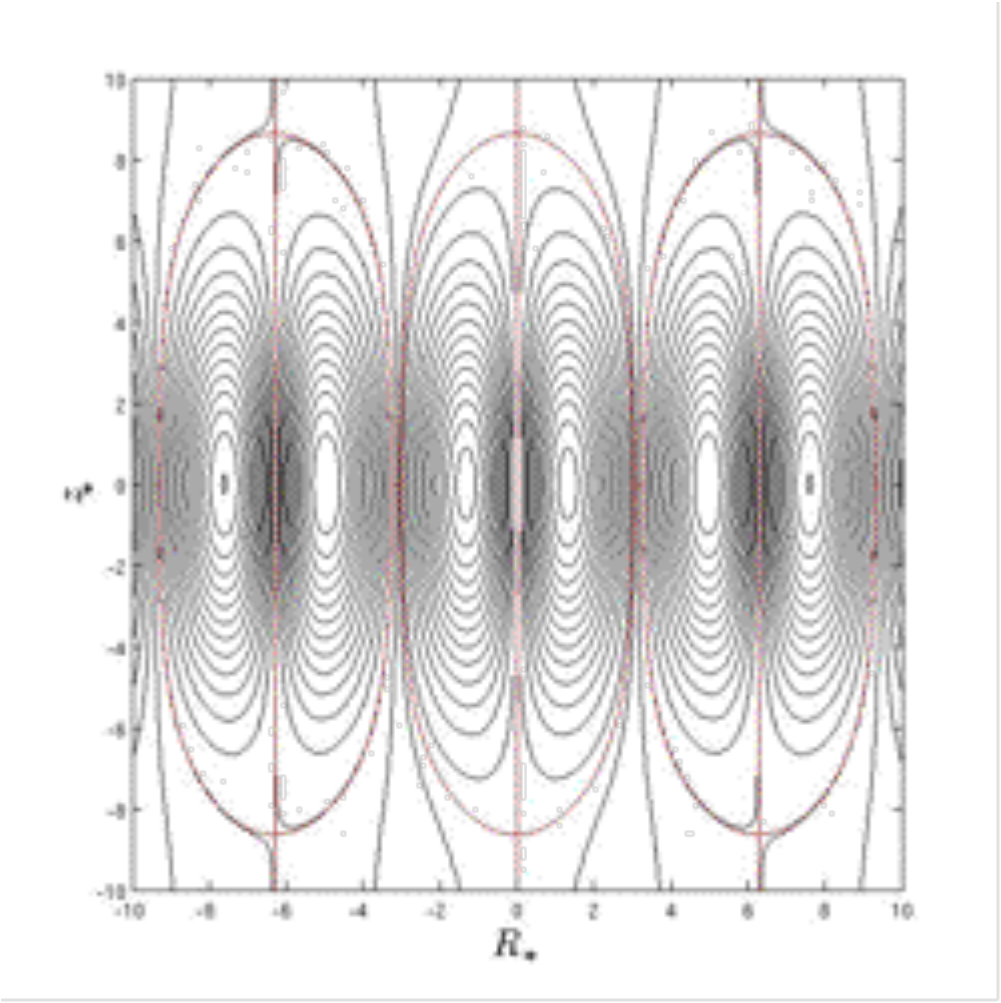

Closed and open magnetic surfaces in the core of a composite disk structure. Here $R_* = \left(R - R_0\right)/\delta_R$.

Ring Pair Solution (B_z-soliton, centered on $R = R_0$)

$$\left(R - R_0\right)^2 \sim \Delta_R^2 \ll R_0^2$$

$$B_z \simeq \left[\frac{1}{\left(1+R_*^2\right)^{3/2}} \exp\left(-\frac{\overline{z}^2}{2}\right)\right] \frac{\psi_1^0}{\Delta_R R_0} \qquad \text{soliton}$$

Here $R_* \equiv \left(R - R_0\right)/\Delta_R$ and $z \equiv z/\Delta_z$

$$\psi \simeq \psi_0\left(R\right) + \psi_1\left(R - R_0,\, z\right), \qquad \left|\psi_1\right| < \left|\psi_0\right|$$

$$\psi_1 \simeq \psi_1^0 \exp\left(-\frac{z^2}{2\Delta_z^2}\right) \frac{R_*}{\left(1+R_*^2\right)^{1/2}}$$

$$B_z^1 \equiv \frac{\psi_1^0}{\Delta_R R_0} > B^0 \equiv \frac{\psi_0}{R_0^2}$$

$$\Delta_R \sim \frac{\psi_0}{B_z^1 R_0} \sim \frac{B^0}{B_z^1} R_0$$

$$\Delta_z^2 \sim \frac{p}{\rho_k^2}$$

$$n \simeq n_0 \exp\left(-\frac{z^2}{\Delta_z^2}\right)\left[\frac{C_0}{\left(1+R_*^2\right)^{3/2}}+\frac{12R_*^2}{\left(1+R_*^2\right)^{7/8}}\right] \Rightarrow \text{ density profile (Ring Pair)}$$

$$B_R \simeq -\frac{\psi_1^0}{R_0\Delta_z}\frac{R_*}{\left(1+R_*^2\right)^{1/2}}\frac{z}{\Delta_z}\exp\left(-\frac{z^2}{2\Delta_z^2}\right) \Rightarrow \text{ (odd) radial component}$$

$$J_\phi \simeq -\frac{c}{4\pi}\frac{\psi_1^0}{R_0}\exp\left(-\frac{z^2}{2\Delta_z^2}\right)\left[\left(\frac{z^2}{\Delta_z^2}-1\right)\frac{1}{\Delta_z^2}+\frac{3}{\left(1+R_*^2\right)^2\Delta_R^2}\right]\frac{R_*}{\left(1+R_*^2\right)^{1/2}}$$ (odd) toroidal current density

Possible driving factors for the relevant current patterns have to be envisioned.

Ring Pairs (soliton solution)

$$\frac{\partial^2}{\partial z^2} \simeq \frac{\partial^2}{\partial R^2} \qquad |R - R_0| < R_0$$

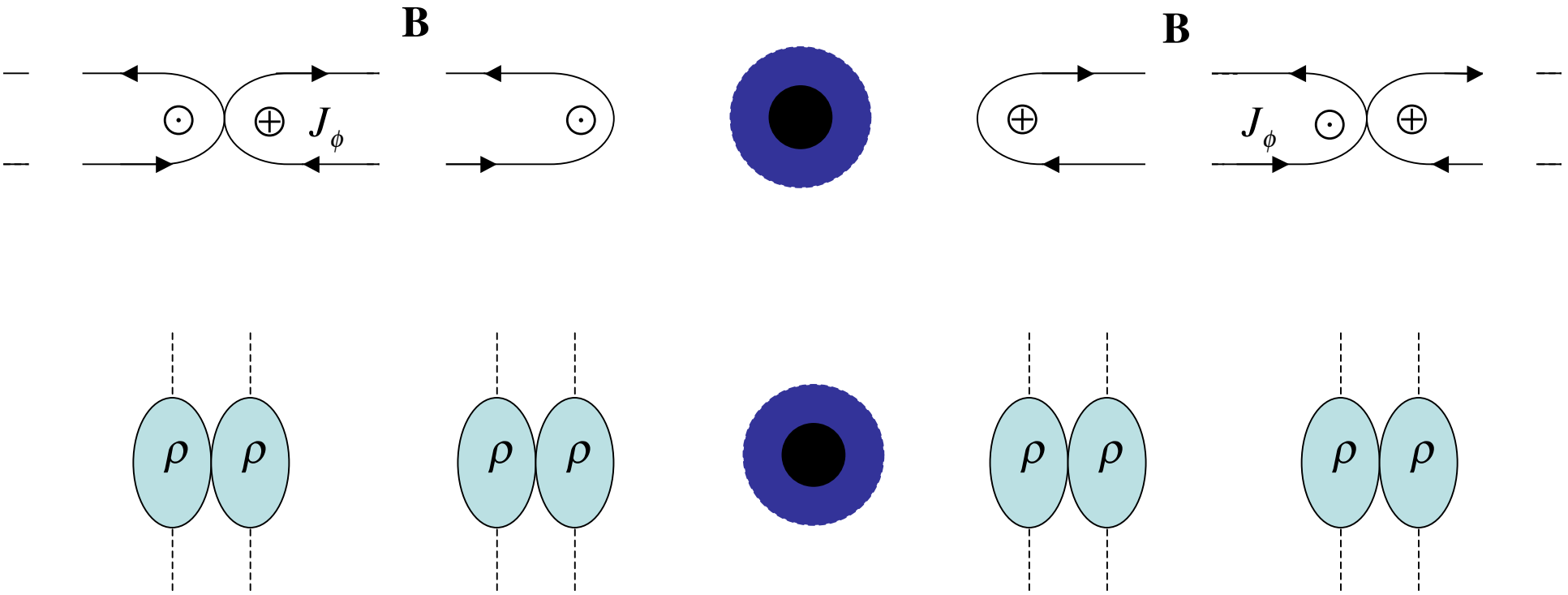

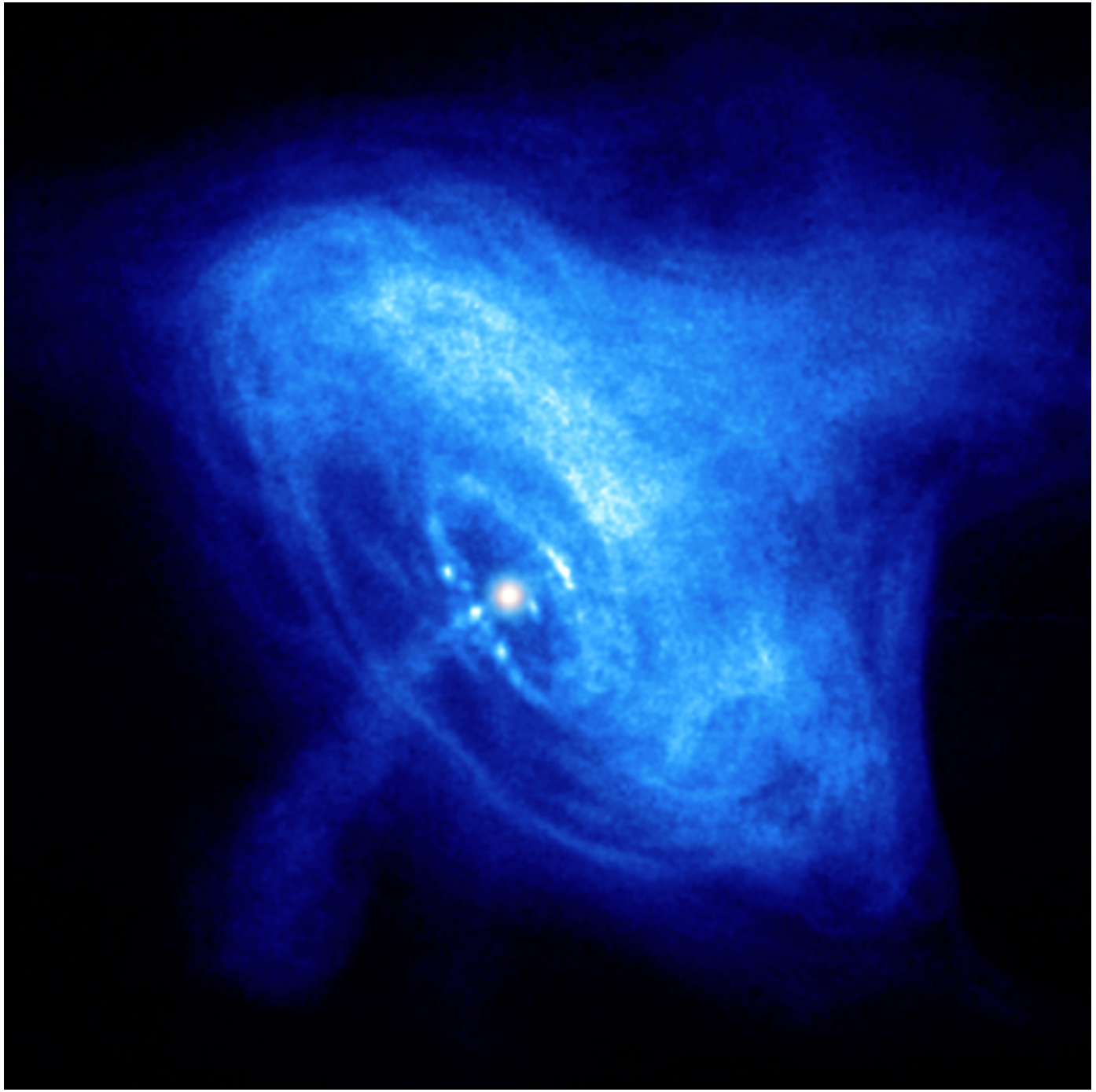

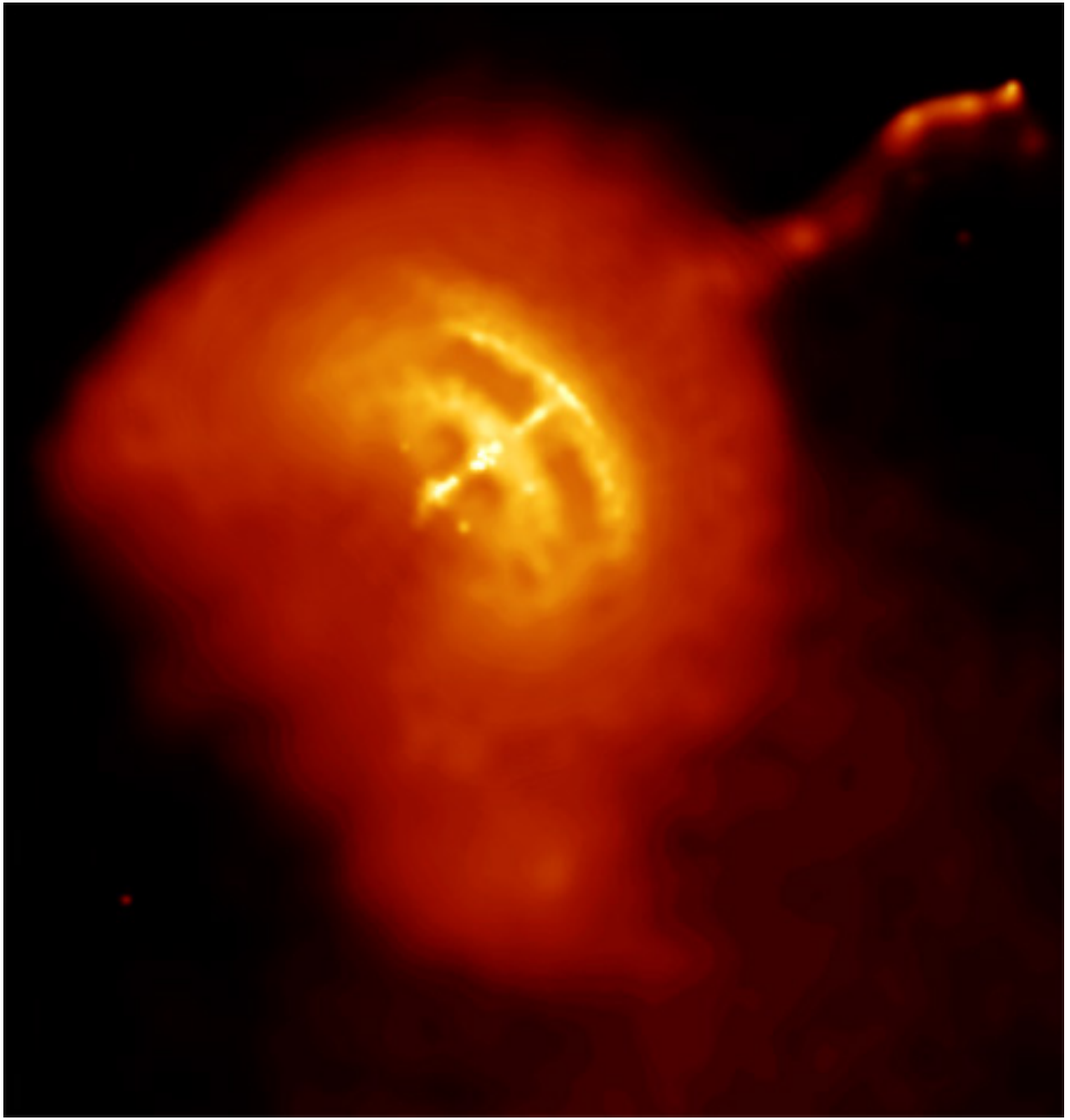

In the case that we consider, the total momentum conservation equation, that includes both the toroidal rotation velocity and the effect of the gravitational field of the a central object, is

$$-\rho\left(\Omega^2 R\mathbf{e}_R + \nabla\Phi_G\right) = -\nabla p + \frac{1}{c}\mathbf{J}\times\mathbf{B} \qquad \text{(I)}$$

where

$$\Phi_G = \frac{GM_*}{\sqrt{R^2+z^2}}, \qquad \nabla\Phi_G \simeq -\frac{V_k^2}{R}\left(\mathbf{e}_R + \frac{z}{R}\mathbf{e}_z\right), \qquad V_k^2 \equiv \frac{GM_*}{R} \equiv \Omega_k^2 R^2.$$

Then we have

$$\mathbf{B}\cdot\nabla p = \rho R\left(\Omega^2 - \Omega_k^2\right)B_R - z\rho\Omega_k^2 B_z \neq 0$$

and if we apply the $\nabla\times$ operator on Eq. (I) we obtain

$$\nabla\times\left(\rho\nabla\Phi_G+\rho\Omega^2R\mathbf{e}_R\right)$$

$$=\mathbf{e}_\phi\left\{\frac{\partial\rho}{\partial z}\left(R\Omega^2+\frac{\partial\Phi_G}{\partial R}\right)+\rho R2\Omega\frac{\partial\Omega}{\partial z}-\frac{\partial\rho}{\partial R}\frac{\partial\Phi_G}{\partial z}\right\}$$

$$=\frac{1}{4\pi R^2}\left[-\frac{2}{R}\left(\Delta_*\psi+I\frac{dI}{d\psi}\right)\mathbf{e}_R+\nabla\left(\Delta_*\psi\right)\right]\times\nabla\psi\,.$$

This can be rewritten as

$$2\Omega_kR\frac{\partial}{\partial z}\left(\rho\delta\Omega\right)+z\Omega_k^2\left(\frac{\partial\rho}{\partial R}+\frac{3}{2}\frac{z}{R}\frac{\partial\rho}{\partial z}\right)$$

$$=\frac{1}{4\pi R^2}\left\{\left[\frac{2}{R}\left(\Delta_*\psi+I\frac{dI}{d\psi}\right)-\frac{\partial}{\partial R}\left(\Delta_*\psi\right)\right]\frac{\partial\psi}{\partial z}+\left[\frac{\partial}{\partial z}\left(\Delta_*\psi\right)\right]\frac{\partial\psi}{\partial R}\right\}\qquad(*)$$

and we call it the "**Master Equation**".

We note that the vertical momentum conservation equation is, considering the expression for F_{Mz} given earlier,

$$0 = -\frac{\partial p}{\partial z} - z\rho\Omega_k^2 - \frac{1}{4\pi R^2}\frac{\partial \psi}{\partial z}\left(\Delta_* \psi + I\frac{dI}{d\psi}\right). \qquad (**)$$

Clearly, we have two equations, (*) and (**), which give $\psi(R, z)$ and $p(R, z)$ for reasonable choices of the density $\rho(R, z)$, the poloidal current function $I(\psi)$, and $\delta\Omega(\psi_1)$.

Is it possible to find profiles that are consistent with known thermal energy balance equations?

Nonclassical Transport and the "Principle of Profile Consistency"

Starting from the experimental observation of temperature and density profiles in magnetically confined plasmas and analyzing the consistency conditions for the plasma-column equilibrium, analytical expressions for the nonclassical energy and particle flows are obtained, and an interpretation of existing experiments is provided.

The problem of understanding the nature of the particle and energy transport processes in magnetically confined plasmas has attracted considerable theoretical and experimental effort in recent years. In fact the theoretical effort has been mostly devoted to numerical simulation of the existing experimental observations, while a relatively simple analytical formulation of this problem would be highly desirable. In this spirit we present a set of criteria that appear to lead to a consistent description of both the electron thermal-energy transport and the particle transport. We label this set of criteria as the "principle of profile consistency." In fact, this is based on assuming that the observed flows of electron thermal energy and particles are those needed to reach a consistent set of radial profiles for the current density, the particle temperatures and the plasma density, while satisfying the equilibrium conditions for the considered plasma column. In addition, we start from the experimental observation that the electron temperature takes on a diffusion-like profile, in impurity-free plasmas, that is

$$T_e \simeq T_{e0} \exp\left(-\alpha_T \frac{r^2}{a^2}\right), \tag{1}$$

a being the plasma column radius and α_T a weak function of r/a. Then, to the extent that the longitudinal resistivity $\eta_\parallel$ is classical, the current density profile is of the form

$$J_\parallel \simeq J_0 \exp\left(-\alpha_D \frac{q_s r^2}{q_0 a^2}\right), \tag{2}$$

Comments Plasma Phys. Cont. Fusion
1980, Vol. 5, No. 6, pp. 261–270
0374-2806/80/0506-0261$04.50/0

This is where a self organization process has to come in, as the experimental evidence for the existence of a radial "profile consistency" (B.C., 1980) of the electron temperature suggests.

In order to proceed further we consider a radial interval $\left|R-R_0\right|<R_0$ around a given radius R_0. Then

$$\Omega \simeq \Omega_k\left(R_0\right)+\left(R-R_0\right)\left.\frac{d\Omega_k}{dR}\right|_{R=R_0}+\delta\Omega$$

and we comply with the isorotation condition $\Omega=\Omega\left(\psi\right)$ defining ψ_z/ψ_{0k} by

$$\left(R-R_0\right)\left.\frac{d\Omega_k}{dR}\right|_{R=R_0}=\Omega_k^0\,\frac{\psi_z}{\psi_{0k}}$$

and ψ_1/B_0 by

$$2\Omega R\delta\Omega \simeq 2\Omega_k^0\left.\frac{d\Omega_k}{dR}\right|_{R=R_0}\frac{\psi_1}{B_0}=-\Omega_D^2\,\frac{\psi_1}{B_0R_0},$$

where $\Omega_D^2\equiv -Rd\,\Omega^2/dR^2=3\Omega_k^2$ is considered to be the "driving factor" for the onset of the magnetic configurations that are analyzed and $\left|\psi_1/\left(B_0R_0^2\right)^2\right|<1$.

On the other hand, for the configurations we shall consider

$$\frac{\partial}{\partial R} \gtrsim \frac{\partial}{\partial z} \gg \frac{1}{R} \quad \text{and} \quad I\frac{dI}{d\psi} \sim \Delta_* \psi \,.$$

In this case $\nabla^2 \simeq \partial^2/\partial R^2 + \partial^2/\partial z^2$ and the Master Equation reduces to

$$\frac{\partial}{\partial z}\left[R\rho\left(\Omega^2 - \Omega_k^2\right)\right] + \Omega_k^2 z \frac{\partial}{\partial R}\rho + \frac{1}{4\pi}\left(B_z \nabla^2 B_R - B_R \nabla^2 B_z\right) \simeq 0\,,$$

that is independent of the toroidal field component.

In this connection we note that the derivation of t he Master Equation is compatible with a pressure tensor of the form

$$\underline{\underline{P}} = p_{th}\underline{\underline{\mathbf{I}}} + p^F \mathbf{e}_\phi \mathbf{e}_\phi$$

Plasma Regimes And Regions

Now, taking into account the characteristics of the observed radiation emission from black hole candidates, we may envision a sequence of three plasma regions developing in the vicinity of a rotating and "active" black hole. These regions differ by the kinds of plasma and magnetic field geometry that are present in them. In particular, we consider

i) a "Buffer Region"

ii) a "Three-regime Region"

iii) a "Structured Low Temperature Region"

The Buffer Region is assumed to be bounded by the Ergosphere and to extend to a distance close to the radius of the marginally stable (e.g. $R_{MS} \simeq 9R_G$) retrograde orbit. This region is assumed to be strongly turbulent. Thus coherent structures originating from external regions should remain excluded from it. The source of energy for this region is considered to be the rotational energy of the black hole.

In the region surrounding to the Buffer Region three plasma regimes can emerge (see following figure). Each regime is characterized both by different particle distributions in velocity space and by different coherent plasma structures. In particular, we may identify

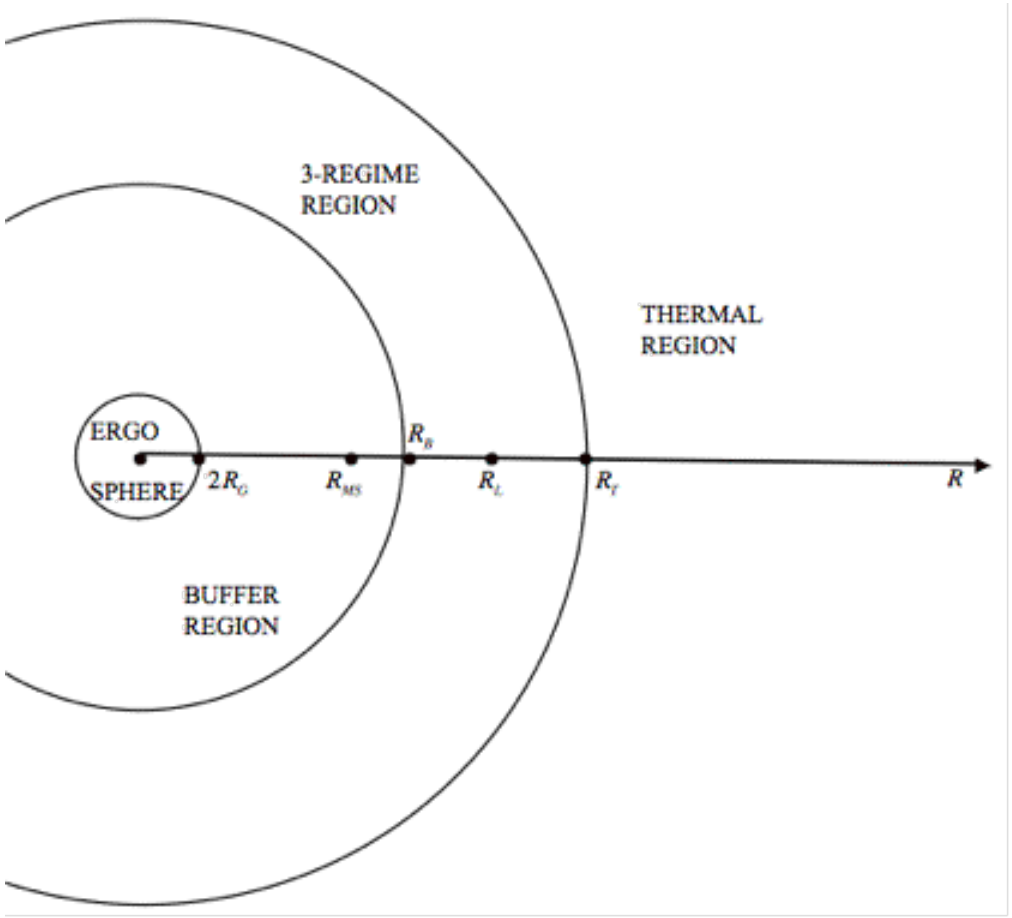

Sketch in the equatorial plane of the plasma regions surrounding a rotating black hole. Here $R_{MS} = 9R_G$ and R_L is the distance at which the maximum amplitude of the spiral modes is localized.

a) an “Extreme” (highly non thermal) Regime in which spiral structures are excited.

b) an “Intermediate Non-thermal” Regime in which plasma ring structures are present and rings are ejected vertically at the inner edge of the region.

c) a “Dissipative Thermal” regime where the ring structure is gradually dissipated within the Region before reaching the Buffer Region.

In fact, it is well established experimentally, on the basis of the characteristics of the radiation emitted from Binary Black Holes, that these can be attributed to 3 states:

i) a “Steep Power Law” (SPL) State,

ii) a “Hard” State,

iii) a Thermal State.

Transitions between states have been observed for the same object.

Tri-dimensional Structures

Referring to the "Extreme Regime" the assumption made in the derivation of the Master Equation that the electron distribution is represented by a scalar pressure p_e can no longer be made. In particular, if the pressure tensor has an anisotropy of the type the Master Equation is no longer valid and we may argue that a two dimensional configuration of a disk structure may not be established. Then dual spiral structures with the same basic characteristics as those described in *A&A* **504** (2009) are envisioned to become dominant. These consist of two spiral channels, one with a relatively high plasma density and one with a low density. The existence of the low density region characterized by relatively low runaway critical fields is consistent with the onset of spiral structures represented by the following density profiles

$$\hat{n} \simeq \tilde{n}_0^0 \frac{z}{\Delta_L^0} \exp\left[-\frac{\left(R-R_2\right)^2}{\Delta_R^2} - \frac{z^2}{\left(\Delta_L^0\right)^2} \right] \sin\left\{ k_R \left(R-R_L\right) - m_\phi \left[\Omega\left(R_L\right) - \phi \right] \right\}.$$

Here R_L is the radial distance around which the mode is localized, Δ_R and Δ_L^0 are the radial and vertical localization distances, respectively, $\Omega\left(R_L\right)$ is the frequency of the plasma rotation around the black hole, and m_ϕ/R_L and k_R are the toroidal and radial mode numbers, respectively. Moreover, $\mathrm{sgn}\left(k_R m_\phi\, d\Omega/dR\right) < 0$ corresponding to trailing spirals.

We note that the expressions for k_R, Δ_R, and Δ_L^0 found from the linearized theory are $k_R \simeq k_0 = \Omega_D/\mathrm{v}_A$, $\mathrm{v}_A^2 = B_0^2/\left(4\pi\rho_0\right)$, where B_0 is the vertical "seed" magnetic field from which the considered perturbation can emerge, ρ_0 is the plasma density on the equatorial plane, $\Delta_L^0 \simeq \left(H_0/k_0\right)^{1/2}$,

$$\Delta_R \simeq \left\{\frac{\gamma_0}{\left|\frac{d\Omega}{dR}\right| m_\phi k_R}\right\}^{1/2} \sim \left(\frac{\gamma_0 R_L}{\Omega_k k_0 m_\phi}\right)^{1/2},$$

γ_0 is the linear growth rate of the unstable mode, $\gamma_0 < \Omega$, $H_0 \equiv c_s / \Omega_k \left(R_L \right)$ and c_s is the local velocity of sound. We observe that accretion should be allowed to proceed at relatively fast rates along the considered spiral structures.

Then we may estimate the spiral co-rotational radius to be at the distance $R_L \simeq \alpha_{MS} R_{MS} + \Delta_R^0$ where $R_{MS} \simeq 9 R_G$, and α_{MS} is an appropriate uncertainty parameter. In addition, we may estimate Δ_R^0 as $\Delta_R^0 \simeq \varepsilon_R \left(R_L H_0 \right)^{1/2}$ where $\varepsilon_R < 1$ is a second uncertainty parameter.

A&A 504, 321–329 (2009)
DOI: 10.1051/0004-6361/200811236

Astronomy & Astrophysics

Spectrum of plasma modes and relevant transport processes in astrophysical disks

B. Coppi

Massachusetts Institute of Technology, Cambridge, Massachusetts, USA
e-mail: coppi@mit.edu

Received 27 October 2008 / Accepted 29 June 2009

ABSTRACT

A simple plasma disk structure imbedded in a magnetic field and in the (prevalent) gravity of a central object is shown to be subject to the excitation of significant axisymmetric and tridimensional modes. The key factors involved in the relevant instability are the plasma pressure vertical gradient and the rotation frequency (around the central object) radial gradient. A modestly peaked vertical profile of the plasma temperature is shown to drive a "thermo-rotational instability" with considerable growth rates. Unstable modes are found as well for "flat" temperature profiles. The tri-dimensional tightly wound spirals that are found have properties that, unlike the familiar galactic spirals, depend on the vertical profiles of their amplitudes. Both radially standing and convective (quasi-modes) spirals are identified. Within the considered spectrum, unstable modes are shown to produce opposing fluxes of particles and thermal energies in the vertical direction. Thus disks with relatively flat vertical temperature profiles can expel particles (winds) from the equatorial plane while transporting thermal energy inward. An effective "diffusion" coefficient, for energy and angular momentum, is derived from the structure of radially convective spiral modes and shown to be consistent with significant radial transport rates.

Key words. accretion, accretion disks – black hole physics – magnetohydrodynamics (MHD) – instabilities – magnetic fields – gravitation

1. Introduction

Identifying the plasma collective modes that can be excited in plasma disk structures (Pringle 1981; Blandford 1976; Lovelace 1976; Coppi & Rousseau 2006) surrounding compact objects such as black holes can be important to explain experimental observations associated with objects of this kind. The geometry of these disk structures (Coppi & Coppi 2001) and their physical parameters, that include in particular the radial gradient of the rotation frequency, the vertical gradients of the particle density and temperature and the effects of the magnetic field in which they are imbedded (Coppi 2008a), determine the characteristics and the spectrum of the modes that can be excited. Novel transport processes of particles and thermal energy in the vertical direction as well as radial transport of angular momentum can be produced by the identified modes. In fact, these processes and the tri-dimensional structure of the spiral modes (Coppi 2008b) that are found can be correlated with important observations connected with black holes (Coppi & Rebusco 2008a). We point out that the properties of the tightly wound spirals that are introduced depend on the vertical profiles of their amplitudes, a feature that is not shared with the better known theory of galactic spirals (Bertin 2000). We note also that the theory presented here for both axisymmetric and tri-dimensional modes include, among others, the physical ingredients of basic modes such as the so called MRI instability (Velikhov 1959; Chandrasekhar 1960; Balbus & Hawley 1991), that is appropriate for different geometries such as cylinders, or the modes that can be excited in well confined plasmas (Coppi & Spight 1978) and can explain the experimentally observed inward transport of particles in connection with the outward transport of plasma thermal energy.

In Sect. 2 the characteristic parameters of the simplest plasma disk structure, imbedded in a vertical magnetic field and surrounding a compact object, are defined in view of the analyses presented in the next sections. In Sect. 3 the basic equations are given for the spectrum of axisymmetric and tri-dimensional normal modes that can be excited in a thin plasma disk. In Sect. 4 the realistic conditions on the density and temperature vertical profiles are examined under which nearly isobaric, weakly compressible modes are found. In Sect. 5 the theory of axisymmetric modes is given and the conditions for their marginal stability are derived. The radial gradient of the rotation frequency and the vertical gradient of the plasma pressure are recognized as the key factors for the excitation of these modes. In particular, when the ratio of the relative gradient of the plasma temperature exceeds the relative gradient of the density by 2/3 a new form of instability (the "thermo-rotational instability") emerges (Coppi 2008a). This is in addition to that of the ballooning modes analyzed by Coppi & Keyes (2003) that are found when the ratio of the gradients mentioned earlier is 2/3 (polytropic profile). In Sect. 6 the transport produced in the vertical direction by the unstable modes described in Sect. 5 is evaluated by the relevant quasi-linear theory. Then the suggestion is made that the outward particle transport (away from the equatorial plane) occurring in the presence of relatively flat temperature profiles be the seed for the observed winds emanating from disks structures surrounding black holes (Elvis 2000). In this case an inward (toward the equatorial plane) flux of thermal energy is produced. The mode growth rates of the unstable modes on which the relevant transport coefficients depend are evaluated by completing the analysis given in Sect. 5. In Sect. 7 the characteristics of the weakly damped oscillatory modes, can be found when the

When the particle distributions in momentum space have a non-thermal component such as that represented by which allows the formation of a composite axisymmetric disk structure in the Three-regime Region, the excitation of spiral modes can be prevented. Then the associated HFQPOs disappear. In addition we may argue that as a result of the interaction between the composite disk structure and the strong turbulence at the edge of the Buffer Region the last couple of plasma rings, carrying oppositely directed toroidal plasma currents that repel each other, could be ejected vertically. Following the arguments given earlier the plasma rings can be expected to "arrive" intermittently with a period related to the onset of the modes that transfer particles from one separatrix to the next. In particular, we may envision that jets results from the ejection of toroids ("smoke-rings") carrying currents in the same (toroidal) directions launched in opposite vertical directions. We also note that experimental observations indicate that jets emerge from evolving disk structures.

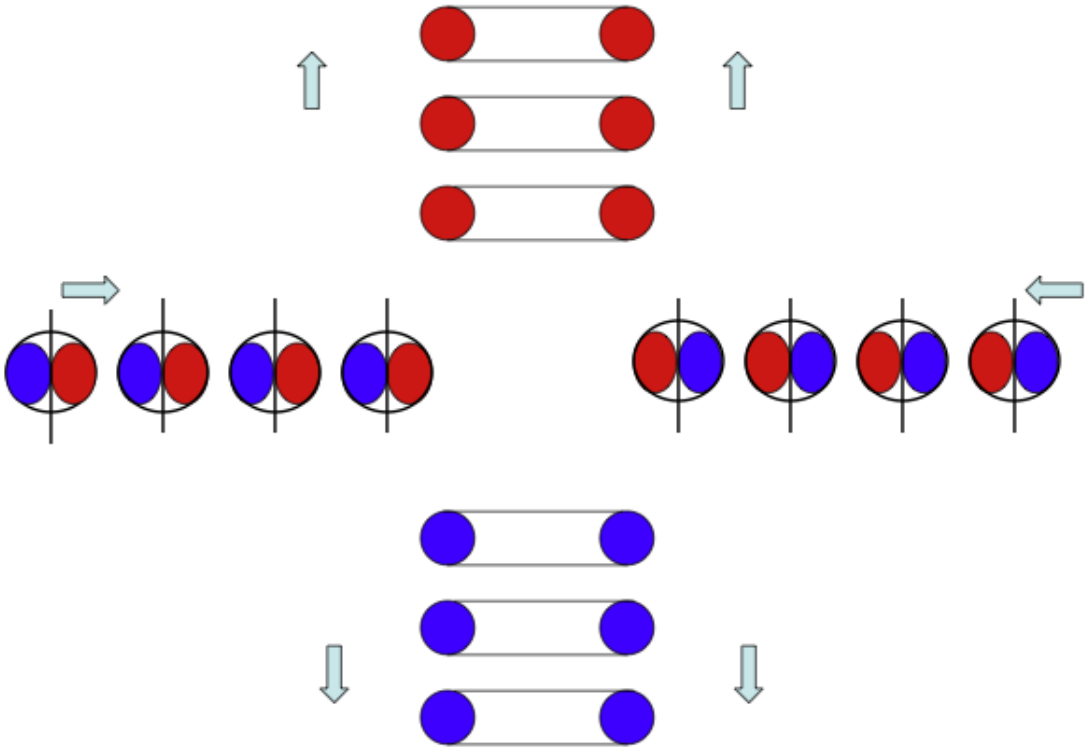

Ring ejection scenario.

In this connection we point out that a recent paper suggests that the power associated with jets is independent of the estimated angular momentum of the black holes with which they are connected. On the other hand it is reasonable to assume that the properties of the Buffer Region and of the plasmas contained in it depend on the black hole rotation. We point out also that the formation and ejection of jets with a purely toroidal magnetic field was proposed and analyzed earlier.

c) In the Dissipative Thermal regime the plasma can reach a relatively high temperature and maintain a thermal distribution as the coherent ring structure is dissipated before reaching the Buffer Region.

Finally, in the outermost region the plasma is considered to be relatively cold and in a well thermalized state. In this region a composite disk structure such as that described earlier is assumed to be well established allowing the (accreting) plasma to flow along successive magnetic separatrices as suggested in the following figure.

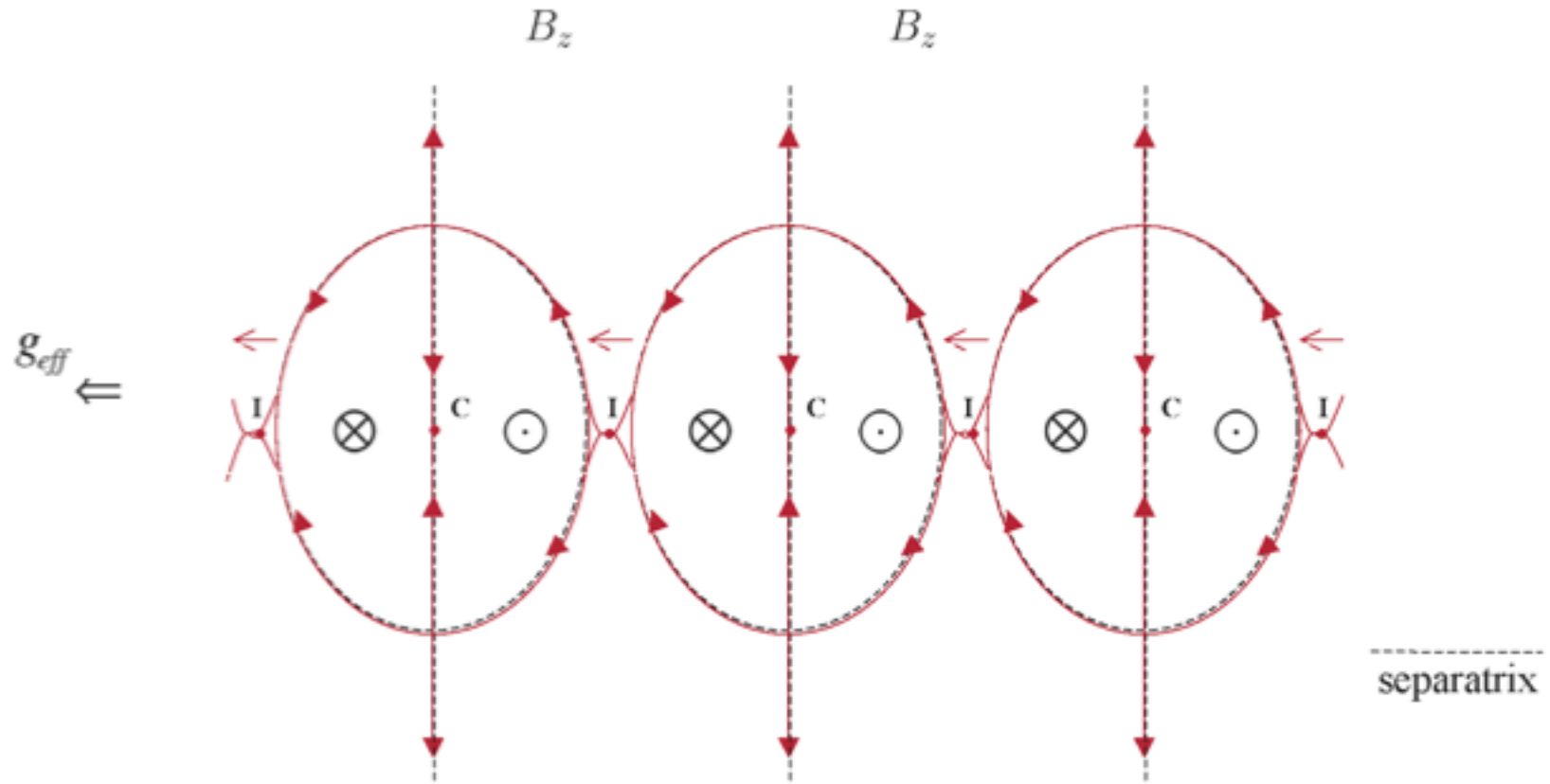

Plasma flow patterns according to the Bursty Accretion scenario.

Low mass X-ray Binaries

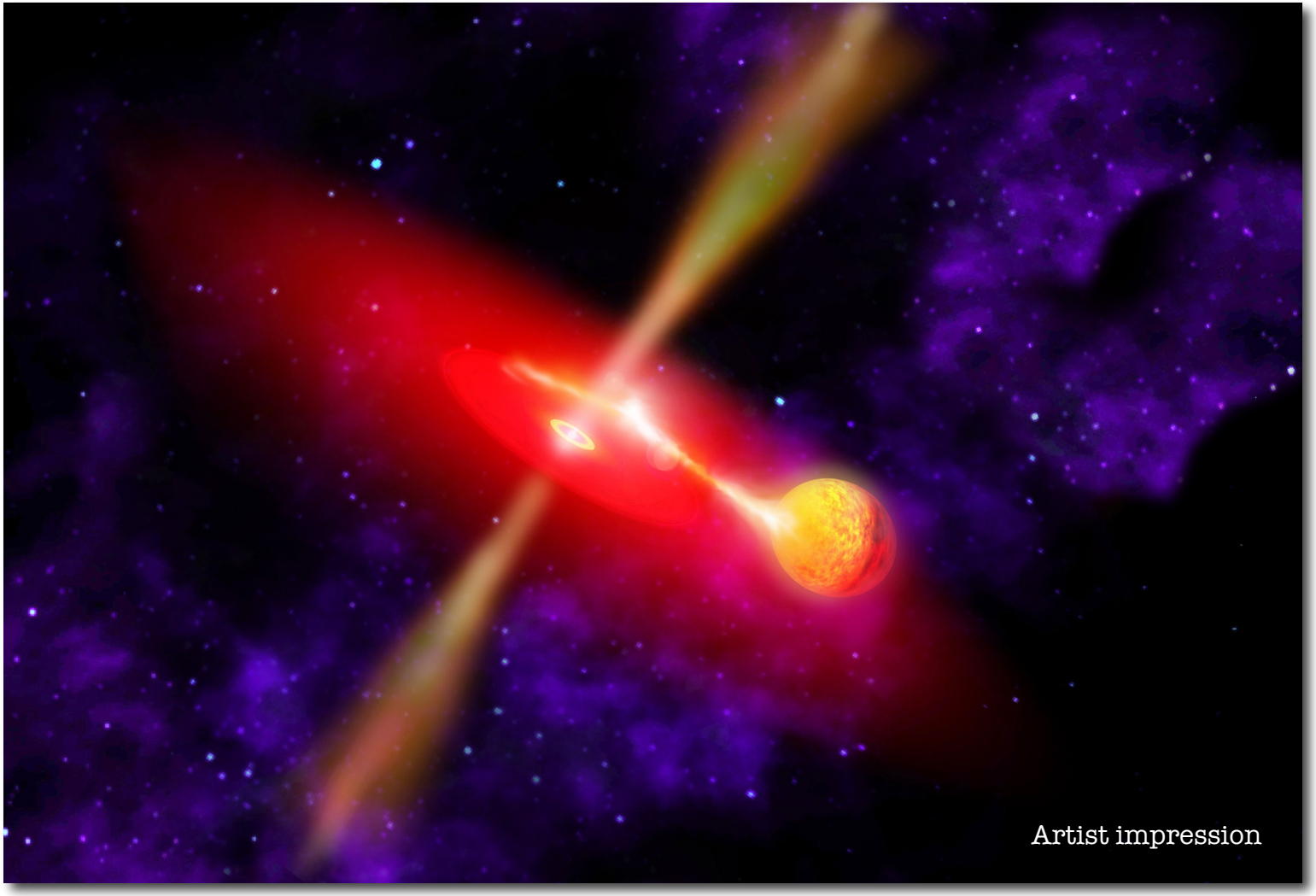

X-ray Observations: Active Spectral States

(Remillard&Mc Clintock 2006)

- **Thermal state** (High/Soft)

  high thermal disc fraction

- **Hard state** (Low/Hard)

  power law (non-thermal emission) - Sometimes jets -

- **Steep power law** (Very High)

  highly non-thermal. Sometimes HFQPOs

High Frequency Quasi Periodic Oscillations (HFQPOs)

- Highly Coherent Peaks in the X-ray power spectra
- 0.1-1200 Hz
  HF-> **few hundred Hz**
- Show up alone OR in pairs OR more
- In **Black Holes**:
  stable **3:2**
- HFQPOs show up in the highly **non-thermal** (steep power law) state
- jets and HFQPOs exclude each other

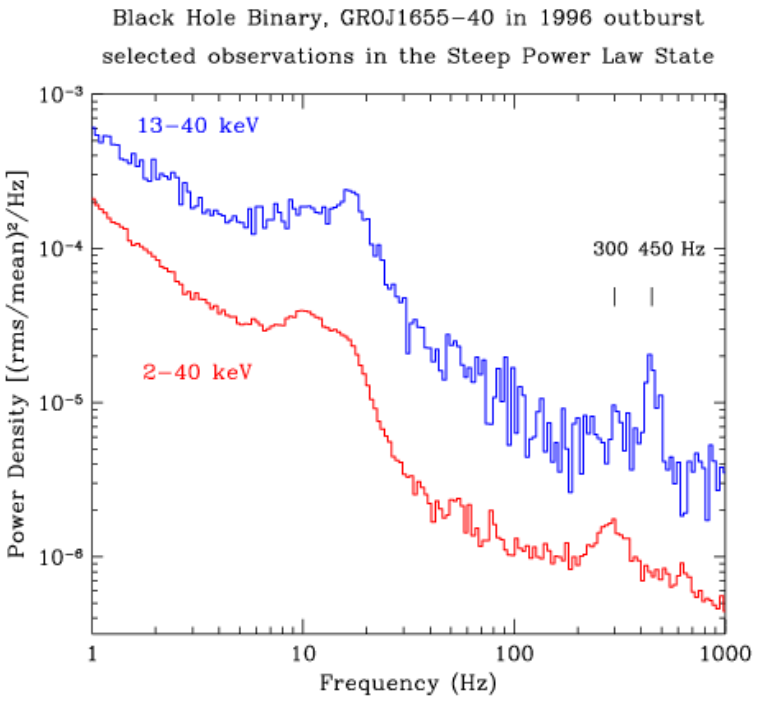

Important Features

•High frequency QPOs lie in the range of ORBITAL FREQUENCIES of free particle orbits just few Schwarzschild radii outside the central source

•The frequencies scale with $1/M$

(e.g, Mc Clintock&Remillard 2004)

Normal Modes in Plasma Accretion Structures (Coppi 2008)

Tridimensional tightly wound spirals excited from a disc embedded in a "seed" vertical magnetic field.

$$\hat{\mathbf{v}}_\phi = \tilde{\tilde{\mathbf{v}}}_\phi\left(R - R_0, z\right)\exp\left(\gamma_0 t - i\omega_0 t + i m_\phi \phi\right)$$ They corotate at $\mathbf{R_0}$

$$\omega_0 = m_\phi \Omega\left(R_0\right)$$

Excitation mechanism: differential rotation and vertical gradients of plasma density and temperature.

3D plasma spirals (trailing)

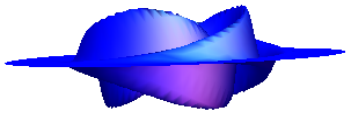

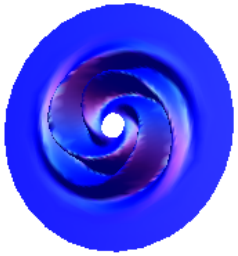

$$\hat{\xi}_z \simeq \tilde{\xi}_z^0 \exp\left[-\frac{(R-R)^2}{\Delta_R^2} - \frac{z^2}{2\,\Delta_z^2}\right] \times$$

$$G_0^0(z)\sin\left\{k_R(R-R_0) - m_\phi\left[\Omega(R_0)t - \phi\right]\right\}\exp(\gamma_0 t)$$

$$\frac{\hat{\rho}}{\rho_0} \simeq -\frac{C_T}{H_0^2} z\tilde{\xi}_z,$$

Δ_R and Δ_z are the radial and vertical localizations

Where are they localized?

(B.Coppi, P.Rebusco and M.Bursa 2011,

in preparation)

We make 2 Assumptions

1) $$H_0 \simeq R_{MS} = \alpha_{MS} R_G$$

H_0 = half height of the disk

$$R_G = \frac{GM_*}{c^2}$$

2) $$\varepsilon^e_{th} \simeq \varepsilon^i_{th} = \alpha_T m_e c^2$$

Hence...

$$R_0 \simeq R_G \left(\frac{\alpha_{MS}^2}{\alpha_T}\frac{m_i}{m_e}\right)^{1/3} \simeq 12.3 \times R_G \times \left(\frac{\alpha_{MS}^2}{\alpha_T}\right)^{1/3}$$

$$R_G = \frac{GM_*}{c^2} \qquad R_s = 2R_G$$

$$\Omega_K(R_0) = \left[\frac{c^2\ R_G}{R_0^3}\right]^{1/2} \simeq \frac{c}{R_G}\left[\frac{\alpha_T m_e}{\alpha_{MS}^2 m_i}\right]^{1/2}.$$

$$\alpha_T = \frac{\varepsilon_{th}^i}{m_e c^2} \qquad \alpha_{MS} = \frac{R_{MS}}{R_s}$$

R_{MS} = radius of marginally stable orbit

M_* = black hole mass

$$\nu = m_\phi \frac{\Omega_K}{2\pi} \simeq \frac{m_\phi}{3} \times \frac{10 M_\odot}{M_*} \times \frac{1}{\alpha_{MS}} \left(\alpha_T \frac{m_p}{m_i}\right)^{1/2} \times 2.2 \times 10^2\ Hz.$$

3:2?

Higher toroidal number m_ϕ modes decay into m_ϕ =2 and m_ϕ =3 modes, consistently with the observed twin peak QPOs spectra with the 3:2 ratio.

Ω_{lower} =2 Ω_K and Ω_{upper} =3 Ω_K

Right Ratio!

$$\frac{1}{\Delta_R^2} = -m_\phi k_R \frac{d\Omega}{dR}\frac{1}{\gamma_0}$$

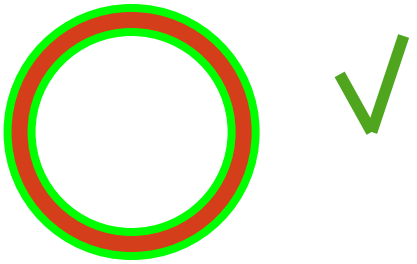

√

Ray-tracing (courtesy of Michal Bursa)

m=2

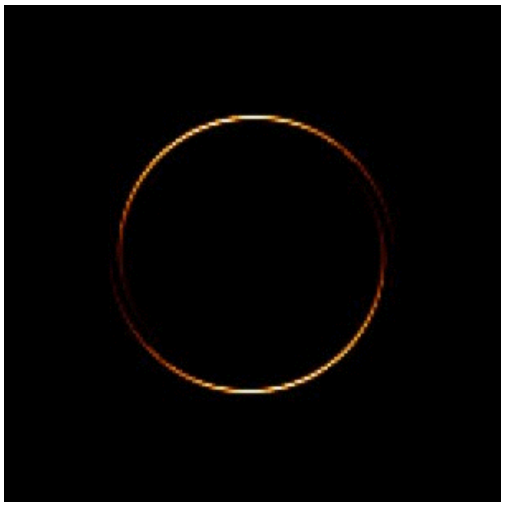

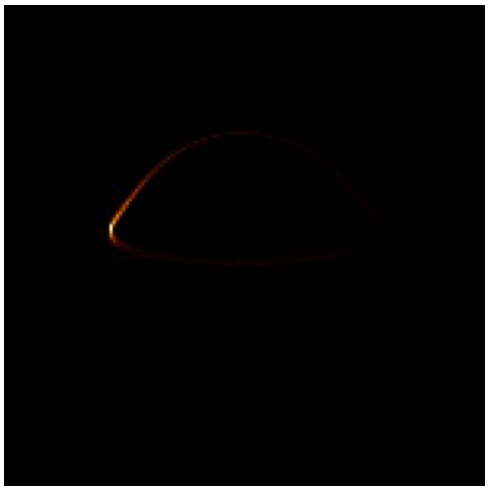

m=3

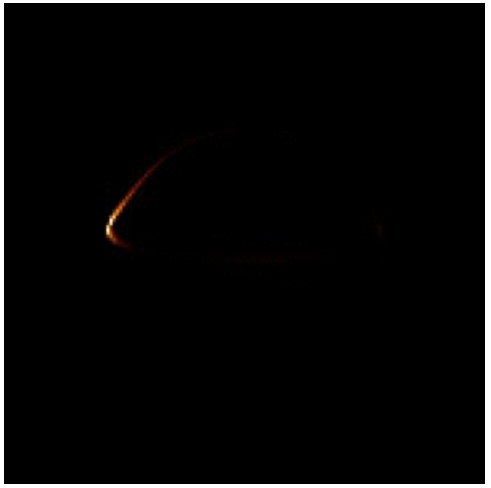

Remarks:

- We propose that the excitation of tri-dimensional spiral modes be considered as the explanation for the emergence of QPO's
- The frequencies of the modes are tied to those of the local rotation frequencies of plasmas around black holes
- A specific physical process for the excitation of the relevant plasma collective modes is given, factor not covered by other proposed theories.
- It is essential to advance the presented theory by dealing, with non-thermal particle distributions in phase space.

GENERAL RELATIVITY CORRECTIONS

The phenomena we consider to guide the presented theory, such as High Frequency Quasi Periodic Oscillations (HFQPOs) are estimated to be related to processes taking place at distances $R \gtrsim 10 R_G$, where $R_G \equiv GM_* / c^2$. Therefore, we can extend the theory given in earlier sections by adopting effective gravitational potentials that include General Relativity effects and can be justified for these distances. In particular, when considering a non-rotating black hole we use the Paczynsky-Wiita gravitational potential

$$\phi_G \simeq -\frac{GM_*}{R - 2R_G}.$$

It is easy to verify that this gives the correct radius (also known as ISCO) for the marginally stable orbit ($R_{MS} = 6R_G$), that the rotation frequency is

$$\Omega_G \simeq \frac{1}{R - 2R_G}\left(\frac{GM_*}{R}\right)^{1/2},$$

and

$$\Omega_D^2 = -\frac{R d\Omega_G^2}{dR} = \frac{3R - 2R_G}{R - 2R_G}\Omega_G^2.$$

As pointed out earlier Ω_D^2 has a prominent role in Eqs. (*) and (***) and is one of the driving factors of the spectrum of modes that can lead to the formation of the considered configurations. As we can see, Ω_G is increased by a factor $3/2$ and Ω_D^2 by a factor 3 for $R = 6R_G$ relative to the Newtonian values.

We observe that, numerically, $R_G \simeq 14.8\left[M_*/\left(10M_\odot\right)\right]$ km and $R_{MS} \simeq 89$ $\left[M/\left(10M_\odot\right)\right]$ km. Considering a disk structure whose height is $2H$, at a given radius $R \gg R_G$, and a mass accretion rate $\dot{M}$ about $10^{-9}\, M_\odot/\mathrm{yr}$, a rudimentary estimate of the plasma density may be made by an average mass conservation equation like $\simeq 2\left[\bar{\bar{\dot{M}}}/\bar{\bar{H}}\bar{\bar{R}}\right]\times\left[5kms^{-1}/\bar{V}_R\right]\times 10^{17}\,\mathrm{cm}^{-3}$ where $\bar{\bar{\dot{M}}} = \dot{M}/\left(10^{-9}\, M_\odot/\mathrm{yr}\right)$, $\bar{\bar{H}} = H/\left(10^3\ \mathrm{km}\right)$, $\bar{\bar{R}} = R/\left(10^4\ \mathrm{km}\right)$. The corresponding Keplerian velocity is $\mathrm{V}_\phi = c\left(R_G/R\right)^{1/2} \simeq 1.2\times 10^4\left(\bar{\bar{M}}/\bar{\bar{R}}\right)^{1/2}\ \mathrm{km\,s^{-1}}$ where $\bar{\bar{M}} = M_*/\left(10M_\odot\right)$.

We note that the radius R_{MS} depends in a significant way on the value of the angular momentum $\mathbf{J} = J\mathbf{e}_z$ that a black hole can have. This is characterized by the dimensionless parameter

$$a_* = \frac{J}{M_* c R_G}$$

with $0 < a_* < 1$, $a_* \to 1$ being the so-called "extreme Kerr" limit. When $a_* \to 1$, $R_{MS} = R_G$ (for a direct orbit), $R_{MS} = 9R_G$ (for a retrograde orbit) while $R_{MS} = 6R_G$ for $a_* = 0$, as indicated earlier. Another important radius associated with the Kerr metric to consider is that of the Ergosphere on the equatorial plane $R_E^0 = 2R_G \equiv R_S$. As is well known, the Kerr metric is

$$ds^2 = -\left(1 - \frac{2R_G r}{r_a^2}\right)(cdt)^2 - (2F_K)(ad\phi)(cdt)$$

$$= \left(r^2 + a^2 + a^2 F_k\right)\sin^2\theta\,(d\phi)^2 + \frac{r_a^2}{\Delta_a^2}dr^2 + r_a^2\,(d\phi)^2,$$

where Boyer-Lindquist coordinates are used, $r_a^2 \equiv r^2 + a^2\cos\theta$, $a \equiv a_* R_G = J/(M_* c)$, $\Delta_a^2 = r^2(1 - 2R_G/r) + a^2$ and $F_K = \left(2rR_G/r_a^2\right)\sin^2\theta$.

In this case we may consider the effective potential for parti cles orbits in the plane $z = 0$, whose radial velocity is given by $\dot{R}^2/(2c^2) + \mathrm{V}_{eff}(R, E_N, L) = E_N/c^2 = \mathcal{E}$, where

$$\mathrm{V}_{eff} = -\frac{R_G}{R} + \frac{L^2/c^2 - 2a^2\mathcal{E}}{2R^2} - \frac{R_G}{R^3}\left(\frac{L}{c} - a\sqrt{\mathcal{E}+1}\right)^2 \qquad (***)$$

and L is the particle specific angular momentum. For circular orbits $\mathrm{V}_{eff} = \mathcal{E}$ and $d\mathrm{V}_{eff}/dR = 0$, give $\mathcal{E}$ and L as functions of R. Then the radius R_{MS} is obtained from $d^2\mathrm{V}_{eff}/dR^2 = 0$. In particular, we may adopt Eq. (***) to add General Relativity corrections to the relevant theory developed in the Newtonian limit.

[1]M. van der Klis and P. Murdin, *Encyclopedia of Astronomy and Astrophysics* (IOP, London, 2000), p. 2380.
[2]R. A. Remillard and J. E. McClintock, Annu. Rev. Astron. Astrophys. **44**, 49 (2006).
[3]D. Psaltis, e-print arXiv:cond-mat/0806, 1531 (2008).
[4]E. F. Taylor and J. A. Wheeler, *Exploring Black Holes* (Addison-Wesley, Boston, 2000), p. F-1.
[5]B. Coppi and F. Rousseau, Astrophys. J. **641**, 458 (2006).
[6]B. Coppi, Astron. Astrophys. **504**, 321 (2009).
[7]B. Coppi, Plasma Phys. Controlled Fusion **51**, 124007 (2009).
[8]B. Coppi, in *Plasmas in the Laboratory and in the Universe*, edited by G. Bertin *et al.* (AIP, New York, 2010), p. 45.
[9]D. Lynden-Bell, Nature (London) **223**, 690 (1969).
[10]J. E. Pringle and M. J. Rees, A&A **24**, 337 (1972).
[11]J. E. Pringle, Annu. Rev. Astron. Astrophys. **19**, 137 (1981).
[12]B. Coppi and M. N. Rosenbluth, Proceedings of the 1965 International Conference on Plasma Physics and Controlled Nuclear Fusion Research, Vienna, 1965.
[13]B. Basu and B. Coppi, Geophys. Res. Lett. **10**, 900, doi:10.1029/GL010i009p00900 (1983).
[14]S. Kato, J. Fukue, and S. Mineshige, *Black-Hole Accretion* (Kyoto Univ. Press, Kyoto, 1998), p. 50.
[15]J. B. Hartle, *Gravity* (Addison-Wesley, San Francisco, 2003), p. 318.
[16]G. I. Ogilvie, Mon. Not. R. Astron. Soc. **888**, 63 (1997).
[17]V. C. A. Ferraro, Mon. Not. R. Astron. Soc. **97**, 288 (1987).
[18]R. H. Cohen, B. Coppi, and A. Treves, Astrophys. J. **179**, 269 (1973).
[19]Chandra X-ray Observatory Center NASA/CXC/SAO. ACIA/HETG Image (2002).
[20]B. Coppi and E. A. Keyes, Astrophys. J. **595**, 1000 (2003).
[21]R. V. E. Lovelace, Nature (London) **262**, 649 (1976).
[22]R. D. Blandford, Mon. Not. R. Astron. Soc. **176**, 465 (1976).
[23]T. E. Strohmayer, W. Zhang, J. H. Swank, I. Lapidus, and J. C. Lochner, Astrophys. J. **469**, L9 (1996).
[24]M. van der Klis, R. Wijnands, W. Chen, F. K. Lamb, D. Psaltis, E. Kuulkers, W. H. G. Lewin, B. Vaughan, J. van Paradijs, S. Dieters, and K. Horne, IAU Circ. **6424**, 2 (1996).
[25]B. Coppi and P. Rebusco, E.P.S. Conference on Plasma Physics, Crete, Greece, 2008.
[26]B. Paczynsky and P. J. Wiita, Astron. Astrophys. **88**, 23 (1980).
[27]R. A. Blandford and R. L. Znajek, Mon. Not. R. Astron. Soc. **179**, 433 (1977).
[28]R. P. Fender, E. Gallo, and D. Russel, Mon. Not. R. Astron. Soc. **406**, 1425 (2010).
[29]R. A. Blandford and D. G. Payne, Mon. Not. R. Astron. Soc. **199**, 883 (1982).
[30]J. Contopoulos, Astrophys. J. **450**, 616 (1995).
[31]N. I. Shakura and R. A. Sunyaev, Astron. Astrophys. **24**, 337 (1973).

THE ASTROPHYSICAL JOURNAL, 179:269–275, 1973 January 1

MAGNETIC CONFIGURATION IN THE NEIGHBORHOOD OF A COLLAPSED STAR

R. H. COHEN, B. COPPI, AND A. TREVES*
Massachusetts Institute of Technology
Received 1972 January 31: revised 1972 May 11

ABSTRACT

It is shown that the magnetic configuration in the neighborhood of a collapsed star with parameters appropriate for models of X-ray stars or pulsars is nearly force-free, with $(\nabla \times \boldsymbol{B})/\boldsymbol{B}$ nonconstant. In the case where the magnetic axis coincides with the rotation axis, a differential equation for the magnetic surfaces is derived. A proper double-expansion technique is used to obtain a significant asymptotic solution of this equation and to derive explicit expressions for the relevant magnetic-field components.

Subject headings: collapsed stars — magnetic fields — pulsars — X-ray sources

I. INTRODUCTION

We consider a rotating collapsed (neutron) star with a magnetic-field configuration that is symmetric about its axis of rotation. We point out that, given the expected high value of the magnetic field, in the vicinity of the polar caps the current flow is nearly parallel to the magnetic field, $\boldsymbol{J} \simeq \alpha \boldsymbol{B}$; hence the field is approximately force-free. In addition, by considering the nature of the electromotive force driving this current and the resultant current flow, one must conclude that α is not constant. For this reason the treatment of force-free field configurations which are found in the literature (Lüst and Schlüter 1954; Chandrasekhar 1956; Chandrasekhar and Kendall 1957; Woltjer 1958; Morikawa 1969) cannot be utilized.

We therefore resort to an asymptotic solution of the general force-free field equations, valid in the vicinity of the rotation axis. In particular we refer, as in the analysis of the equilibrium of laboratory plasmas (Solovev and Shafranov 1970), to the magnetic surfaces of the considered configuration. These surfaces are labeled by the streaming function Ψ which satisfies the equation $\boldsymbol{B} \cdot \nabla \Psi = 0$. Our solution enables us to give explicit expressions for the magnetic surfaces and field lines, and to formulate a precise criterion to establish limits for the current which flows through the star surface. Here we summarize our analysis, while a more detailed treatment of the same problem will be published elsewhere (Cohen, Coppi, and Treves 1972).

We assume that the collapsed star under consideration is surrounded by a plasma-sphere and distinguish two regions: an active region near the symmetry axis, where poloidal currents can flow, and an inactive equatorial region where the plasma co-rotates with the star. The existence of poloidal currents in the active region results from slippage of the plasma with respect to the magnetic field; this slippage can be associated with the finite plasma resistivity and with relativistic effects and produces an electromotive force. The two regions are separated by the magnetic surface which intersects the star at colatitude θ_c; if we assume that the poloidal magnetic field is dipolar, we find that θ_c is of order $(\omega_0 a/c)^{1/2}$ where ω_0 is the angular velocity of the star and a its radius.

We consider a region well inside the speed-of-light cylinder and write the equation of

* Permanent address: Istituto di Fisica dell'Università, Milano, Italy.

which is independent of r. The condition that the first, second, and fourth terms of equation (13) be dominated by $(4\chi/\hat{r}^3\Psi_c)\Psi_{xx}^{(1)}$ gives, respectively,

$$\sin^2\theta \ll 8\,, \qquad \sin^2\theta \ll 2\,, \qquad \sin^2\theta \ll \tfrac{4}{3}\,,$$

which together with expression (23) may be written

$$\sin^2\theta \ll \min\left[(\Psi_c/\hat{\alpha}_M)^{2/3}, \tfrac{4}{3}\right]. \tag{24}$$

Our solution is valid, then, as long as both the above condition and the force-free field approximation hold.

IV. MAGNETIC SURFACES AND FIELD LINES

A point (r, θ, ϕ) is related to a point (a, θ_0, ϕ_0) at the surface of the star on the same magnetic surface by the equation $\Psi(r, \theta) = \Psi(a, \theta_0)$, or equivalently, by $\Psi(\hat{r}, \chi) = \Psi(\hat{r} = 1, \chi_0)$ where $\chi_0 = (\sin^2\theta_0)/\Psi_c$. One may use the latter form of this equation to obtain an expression for the magnetic surfaces in polar coordinates. Writing $\Psi(\hat{r}, \chi) = \Psi^{(0)} + \Psi^{(1)} \equiv \Psi_c\chi + \Psi^{(1)}(\hat{r}, \chi)$, the preceding equation gives

$$(\chi - \chi_0) = [\Psi^{(1)}(\hat{r} = 1, \chi_0) - \Psi^{(1)}(\hat{r}, \chi)]/\Psi_c$$

implying that $\chi - \chi_0$ is of order $(\Psi^{(1)}/\Psi_c) \lesssim (\Psi^{(1)}/\Psi^{(0)})$. We may obtain an expression for $(\chi - \chi_0)$ correct to first order in $(\Psi^{(1)}/\Psi_c)$ by simply replacing $\Psi^{(1)}(\hat{r}, \chi)$ by $\Psi^{(1)}(\hat{r}, \chi_0)$ in the above equation. Assuming that the separated form (16) is applicable, so that $\Psi^{(1)} = -(\hat{r}^3\Psi_c/4)\psi(\chi)$, the result may be expressed in the form

$$\frac{\sin^2\theta}{\hat{r}} = \sin^2\theta_0 + \tfrac{1}{4}\Psi_c\psi(\chi_0)(\hat{r}^3 - 1)\,. \tag{25}$$

For a current distribution corresponding to $\hat{\alpha}$ chosen as in equation (11), the coefficient of $(\hat{r}^3 - 1)$ is positive for all magnetic surfaces in the range of our approximations; θ increases with r along a magnetic surface faster than for a dipole field. Since field

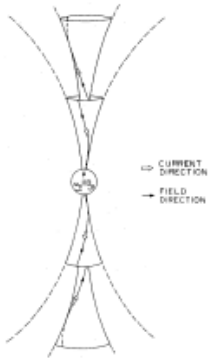

FIG. 1.—Sketch of magnetic surfaces and field lines

ANNALS OF PHYSICS **119,** 97–116 (1979)

Magnetic Equation for a Rotating Neutron Star

B. COPPI AND F. PEGORARO*

Physics Department, Massachusetts Institute of Technology, Cambridge, Massachusetts 02139

Received July 19, 1978

The magnetic configuration in the plasma-sphere surrounding a neutron star is described in terms of a model equation that is constructed to be valid from the surface of the star to distances of the order of the light speed cylinder and beyond. Significant asymptotic solutions of this equation, that are valid in limited regions around the star, are presented.

1. INTRODUCTION

One of the problems that have to be dealt with when considering possible models for pulsars concerns the macroscopic properties of the plasma that can surround a rotating neutron star. The high magnetic field that is associated with this type of star and the relatively high frequency of rotation that is appropriate for pulsar models are the most important parameters determining the nature of the plasma-sphere surrounding the star.

In the following sections we give an analytical procedure, for a fluid-like description of this plasma-sphere, that leads to solve an equation in the scalar labeling the (magnetic) surfaces of the relevant magnetic configuration. A number of important effects, that it is necessary to consider when analyzing the possible types of plasma flow and magnetic field configurations at distances of the order of or larger than the radius of the "light-speed-cylinder," are discussed and taken into account in the above mentioned magnetic equation. These include the fact that the plasma does not strictly corotate with the star and that its motion is not "frozen-in" everywhere with the magnetic field, the influence of the gravitational and of the centrifugal forces, and the effects of a "braking" force on the plasma resulting from the emission of radiation and particles. Moreover, the braking mechanism has to satisfy the condition that the star rate of energy loss be equal to the rate of angular momentum loss times the frequency of rotation. For the sake of simplicity, a two dimensional model is analyzed assuming that the axis of rotation coincides with that of the magnetic field configuration (Goldreich and Julian, 1969). This magnetic configuration depends upon two expansion parameters which are related to the portion of star surface from which poloidal currents are drawn, and to the ratio between the toroidal and the poloidal magnetic field at the star surface. An estimate of these parameters can be obtained

* Permanent address: Scuola Normale Superiore, Pisa, Italy.

0003-4916/79/050097-20$5.00/0

respectively, where $\theta_c \simeq \psi_c^{1/2}$ as follows from Eq. (3.1). Therefore,

$$\Phi \neq 0 \text{ if } 0 < \psi < \psi_c \quad \text{and } \Phi = 0 \text{ if } \psi_c \leqslant \psi. \tag{3.4}$$

In addition, on each of the polar caps Φ is assumed to be a function of ψ only, as there is no braking force close to the star. Two regions around the star are thus postulated, an active and an inactive one (see Fig. 1). The active region extends from the polar caps ($r = a$, $\psi < \psi_c$) to a "critical surface" beyond which the motion of the plasma is no longer tied to the star magnetic field. Current is drawn from the polar caps along constant Φ-surfaces which, in the neighborhood of the star, coincide with magnetic surfaces. The inactive region is assumed to be bounded by the magnetic surface $\psi = \psi_c$ that is tangent to the critical surface. In addition, it is reasonable to assume that inside the inactive region there is no poloidal current so that the magnetic configuration, in a region relatively close to the star, is that of a dipole corotating with it. The braking of the plasma, which is connected with the rate of energy and

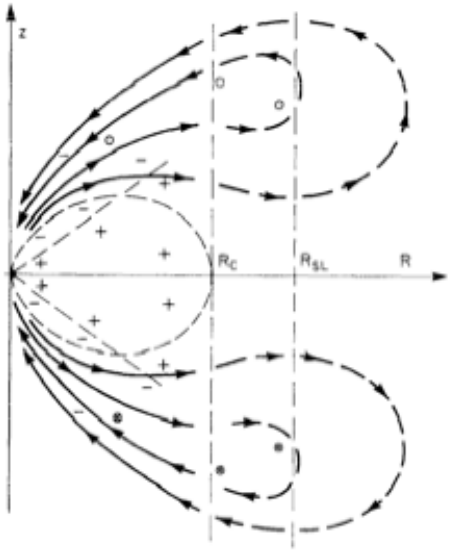

FIG. 1a. Current distribution in the rotating star magnetosphere. The star is indicated by the small circle around the origin. The light broken curve shows the boundary between the active and the inactive region while the straight broken line separates the region of positive charge (+) from the region of negative charge (−) close to the star. The current flow is indicated by heavy lines, solid for $R < R_c$ and broken for $R > R_c$ where the circuit closes. The orientation of the toroidal magnetic field in the active region is symbolized by crossed ⊗ and dotted ○ small circles. The dipole magnetic moment and the angular velocity of the star have been assumed to point in the same direction.